Title	Emergence of swing-to-stance transition from interlocking mechanism in horse hindlimb
Author(s)	Miyashita, Kazuhiro; Masuda, Yoichi; Gunji, Megu et al.
Citation	2020 IEEE/RSJ International Conference on Intelligent Robots and Systems (IROS). 2021, p. 7860-7865
Version Type	AM
URL	https://hdl.handle.net/11094/90043
rights	© 2021 IEEE. Personal use of this material is permitted. Permission from IEEE must be obtained for all other uses, in any current or future media, including reprinting/republishing this material for advertising or promotional purposes, creating new collective works, for resale or redistribution to servers or lists, or reuse of any copyrighted component of this work in other works.
Note	

Emergence of Swing-to-Stance Transition from Interlocking Mechanism in Horse Hindlimb*

Kazuhiro Miyashita[1], Yoichi Masuda[1], Megu Gunji[2],
Akira Fukuhara[3], Kenjiro Tadakuma[4], and Masato Ishikawa[1]

Abstract— The bodies of quadrupeds have very complex muscle-tendon structure. In particular, it is known that in the horse hindlimb, multiple joints in the leg are remarkably interlocked due to the muscle-tendon structure. Although the function of these interlocking mechanisms during standing has been investigated in the field of anatomy, the function related to the emergence of limb trajectory during dynamic walking has not been revealed. To investigate the role of the interlocking mechanism, we developed a robot model imitating the muscle-tendon arrangement and the dynamics of a horse hindlimb. In the walking experiment, the robot autonomously generated a limb trajectory with a smooth transition between the swing phase and the stance phase by simply swinging the hip joint with sinusoidal input. Moreover, we compared the joint angles between successful and failed walking. The compared results indicate that the extension of the fetlock joint after hoof touchdown plays the crucial role in emergence of a function of supporting body.

I. INTRODUCTION

Quadrupeds can generate adaptive limb trajectories according to the locomotion speed and environmental conditions. For example, elephants and horses generate different limb trajectories when walking and running [1], [2], [3]. Cats also generate different limb trajectories when going up or down slopes than when walking on level ground [4], [5].

In the field of robotics, autonomous generation of limb trajectories has been achieved by the passive walker [6] that can walk downslope using only gravity and by a pneumatic musculoskeletal robot [7] that is based on the reflex mechanisms in quadrupeds. These studies have demonstrated that the limb trajectories, which were previously given arbitrarily by the robot designers, can be naturally generated from the dynamic interaction between the robot body and the environment. However, the ability of these robots to generate

[1]Department of Mechanical Engineering, Osaka University, 2-1 Yamadaoka, Suita, Osaka 565-0871, Japan k_miyashita@eom.mech.eng.osaka-u.ac.jp
[2]National Museum of Nature and Science, Tokyo, 4-1-1 Amakubo, Tsukuba-shi, Ibaraki 305-0005, Japan
[3]Research Institute of Electrical Communication, Tohoku University, 2-1-1 Katahira, Aoba-ku, Sendai 980-8577, Japan
[4]Graduate School of Information Sciences, Applied Information Sciences, Tohoku University 6-6-01 Aramaki Aza Aoba, Aoba-ku, Sendai-shi, 980-8579, Japan
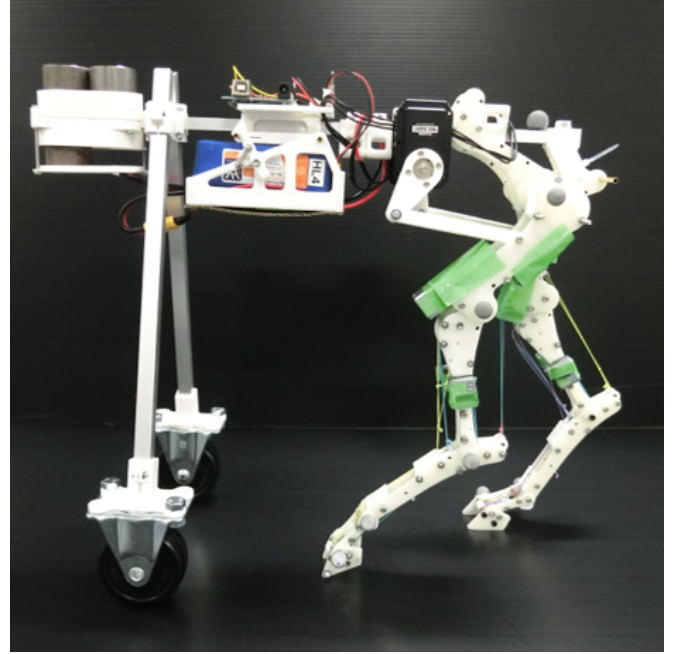
Fig. 1. Robot model imitating musculoskeletal structure of horse hindlimb.

limb trajectories remains very limited, far from the ability of animals to stabilize walking postures and adapt according to rough ground surfaces. We believe that the cause of the difference of ability is hidden in the gap of basic design principle of the body structure between the robots and the animals. Therefore, in this study, we focus on the complex muscle-tendon structure, one of the mechanisms observed in animals but not in robots.

In this study, we focus on horses, which have been well investigated in the field of anatomy and biology. There are various interlocking mechanisms in the legs of horses that are relevant to the emergence of the limb trajectory [8]. One of the anatomical features of the horse hindlimb is called the reciprocal apparatus [9], [10]. This apparatus enables the stifle (knee) and the hock (ankle) joint to flex and extend simultaneously. Furthermore, horses can support their weight by tendons and ligaments in the legs by simply putting the tip of the hoof on the ground [9], [11]. This interlocking mechanism is known as stay apparatus, and it is also assumed to contribute to the weight support of walking horses. Although it has long been suggested that these interlocking
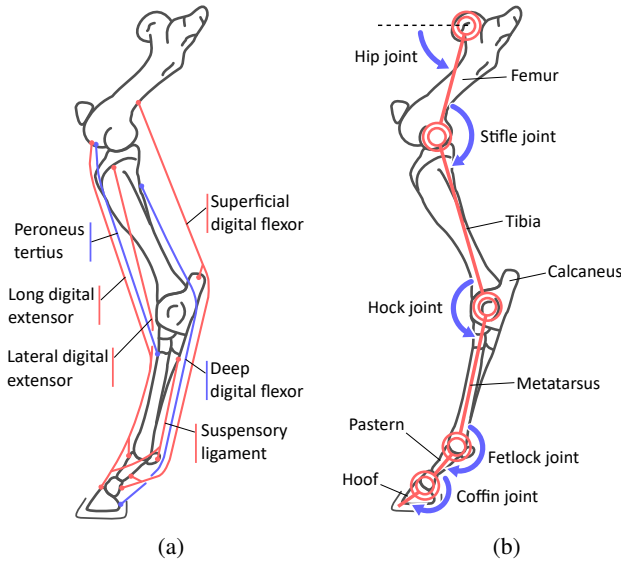
Fig. 2. Simple musculoskeletal structure in the horse hindlimb. (a) shows muscle-tendon structure. (b) shows link structure and bone names. The blue arrows indicate extending direction.

Fig. 3. The movement of the interlocking mechanism in the horse hindlimb.

mechanisms are involved in the generation of limb trajectories, detailed mechanisms have not been clarified owing to dynamic and complex interactions with muscles, tendons, skeletons, and the environment. In addition, it is difficult to investigate the function of the interlocking mechanisms in the leg during walking because of various restrictions in experiments using real horses. Therefore, in this study, we develop a robot model that imitates the muscle-tendon structure of a horse hindlimb, as shown in Fig. 1, and clarify the emergence mechanism of a horse's limb trajectory via a constructive approach. The discovery in this study is that the trajectory of a horse hindlimb (limbs support the body firmly during stance phase and away from ground during swing phase) can be generated from the interaction between the limb with interlocking mechanism and the ground. Moreover, the compared results between successful and failed walking indicate that the extension of the fetlock joint after hoof touchdown plays the crucial role in emergence of a function of supporting body.

II. MECHANISMS IN THE HORSE HINDLIMB

In this study, we focus on the muscle-tendon structure in a horse hindlimb. In this section, we introduce the interlocking mechanisms consisting of the muscle-tendon structure. Fig. 2 illustrates the musculoskeletal structure in the horse hindlimb.

First, we explain the movement of the limb when the stifle joint flexes by fixing the tibia and moving the femur as shown in Fig. 3(a). When the stifle joint flexes, the peroneus tertius muscle, which begins on the bottom of the femur, is pulled and the hock joint also flexes. As a result, the calcaneus protrudes, the deep digital flexor muscle is pulled, and the coffin joint flexes. In addition, because the range of motion of the coffin joint is limited, the fetlock joint also flexes. Due to this interlock, only some joints' flexion leads to the flexion
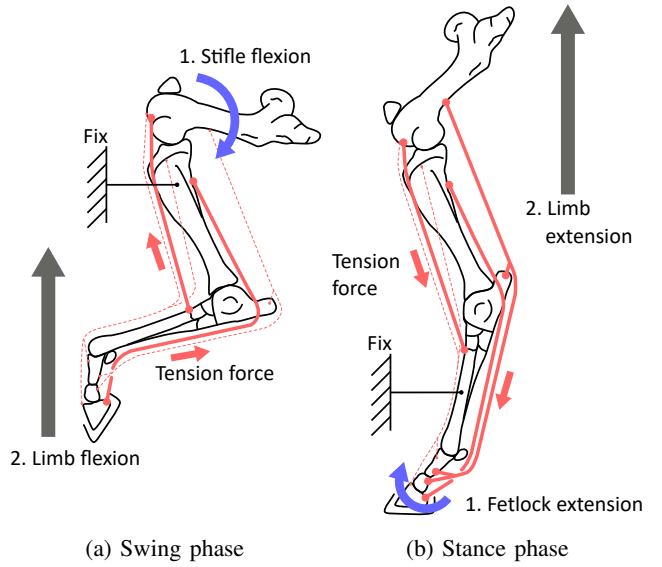
of entire limb. From this, we expect that the limb would rise higher and be prevented from tripping to the ground during the swing phase.

We thereafter explain the movement of the limb when the fetlock joint flexes by fixing the metatarsus and moving the pastern as shown in Fig. 3(b). When the fetlock joint extends, the deep digital flexor, which is inserted into the rear edge of the hoof, is pulled and the hock joint also extends. Simultaneously, the stifle joint extend by the peroneus tertius. We expect that the limb is extended and the body is supported during the stance phase because the joints are forced to extend while the ground reaction force on the hoof extends the fetlock joint. In other words, the function of the limb is switched by the interaction between the limb with interlocking mechanism and the ground.

III. ROBOT DESIGN

In this section, we describe the developed hindlimb model reproducing the interlocking mechanisms shown in section II. Thereafter, we explain the design of the developed robot with two hindlimb structures and its control system.

A. Developed hindlimb model

Fig. 4 shows the overview of the developed hindlimb model and the detailed structure of the origin of tendons. We designed each link so that the dimension ratio of each link in the axial direction was equivalent to that of the real horse's. We adopted five joints (hip, stifle, hock, fetlock, and coffin joints) and regarded all joints as hinge joints moving to the sagittal plane.

In the horses, the distal part of the limb muscles usually become long tendons [12]. In other words, the passive elements by tendons may be dominant in the distal part of the limb. Therefore, we reproduce the connection between bones through muscles and tendons using polyethylene wires, and we do not actively control muscles below the lower limb. Moreover, we connect the polyethylene wires and bones via
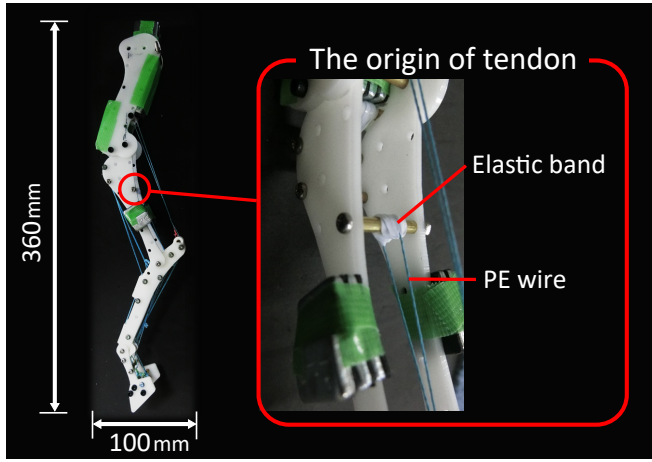
Fig. 4. Overview of the hindlimb model. The left figure shows the extending hindlimb model. The right figure shows the structure of the origin of tendons.
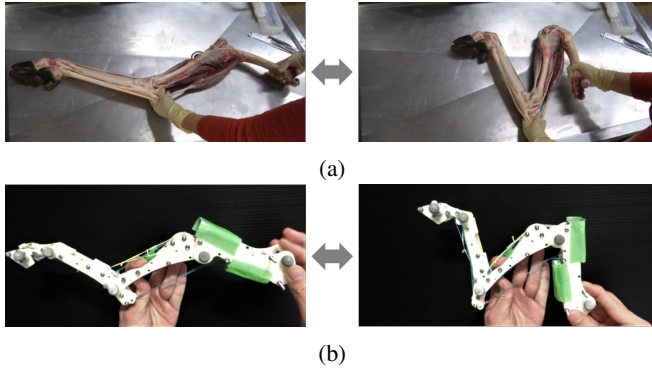

(a)

(b)

Fig. 5. The movement of (a) real reindeer and (b) robot hindlimb. The left figures indicate extending limbs. The right figures indicate flexing limbs.
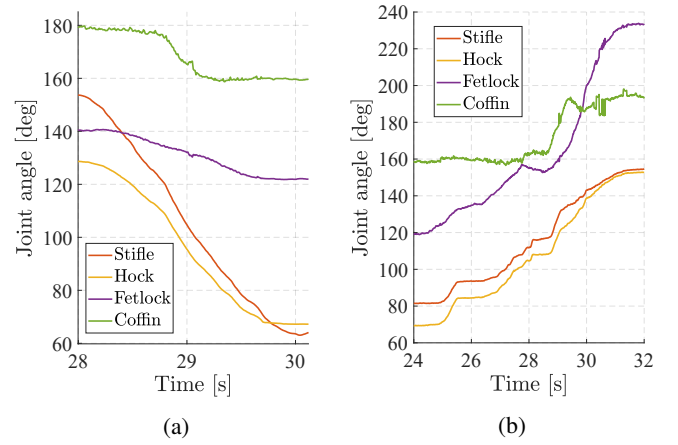

(a)   (b)

Fig. 6. The joint angles when (a) the stifle joint is flexed and (b) the fetlock joint is extended by hand.
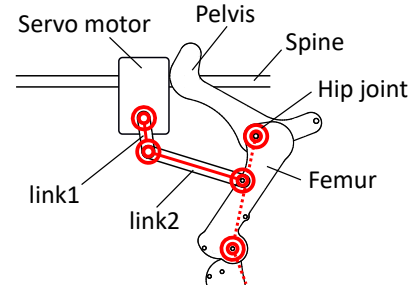
Fig. 7. The link structure around hip joint of the robot.

elastic bands at the origin of all muscles and the insertion of some muscles to reproduce the elasticity of tendons. We referred to the literature [9], [13] for the axis of rotation of the joints and the origin together with the insertion of the muscles.

Fig. 5 shows the comparison between the developed hindlimb model and a real reindeer hindlimb, which is a species of the ungulate and has the same interlocking mechanism as horses. The left figures are for extension and the right figures are for flexion. The figure shows that the stifle, hock, and fetlock joints flex and extend simultaneously. In addition, we measured the motion of each joint angle when performing the same operation by hand as in Fig. 3, to verify the interlocking mechanism. Fig. 6(a) shows the joint angles when the femur is moved and the stifle joint flexes. When the stifle joint flexes, the other joints flex simultaneously. Fig. 6(b) shows the joint angles when the pastern is moved and the fetlock joint extends.

We expect that the function of the limb switches because of these interlocking mechanisms between the swing phase and the stance phase.

B. Body design

In order to evaluate the interlocking mechanism in the hindlimb model, we developed the robot body with the hindlimb model (Fig. 1).

The robot has two hindlimbs and fore-wheels. The spine of traveling horses during walking is almost rigid [11], so we designed the spine of the robot with a rigid beam. We fixed the pelvis of the robot to the spine because the pelves of horses hardly rotate on the sagittal plane [8]. We attached the hindlimb model to the pelvis so that it could rotate around the hip joint.

We use two servo motors (DYNAMIXEL MX-64AT, ROBOTIS) for driving the hip joints. We connect the servo motor to the femur via the link structure as shown in Fig. 7. The distance between the forelimbs and the hindlimbs and the distance between the hindlimbs mimicked part of the real horses. Furthermore, we attached a weight to the head of the robot to match the center of gravity of the entire robot with the real horses.

C. Periodic motion of hip joint

The hip joint of real horses shows a sinusoidal motion [14]. Therefore, in this study, we performed feedforward control with the servo motors so that the femur made a sinusoidal motion. In addition, we controlled the right hindlimb and the left hindlimb to move in opposite phases, as we imitated the movement of the walking horses.

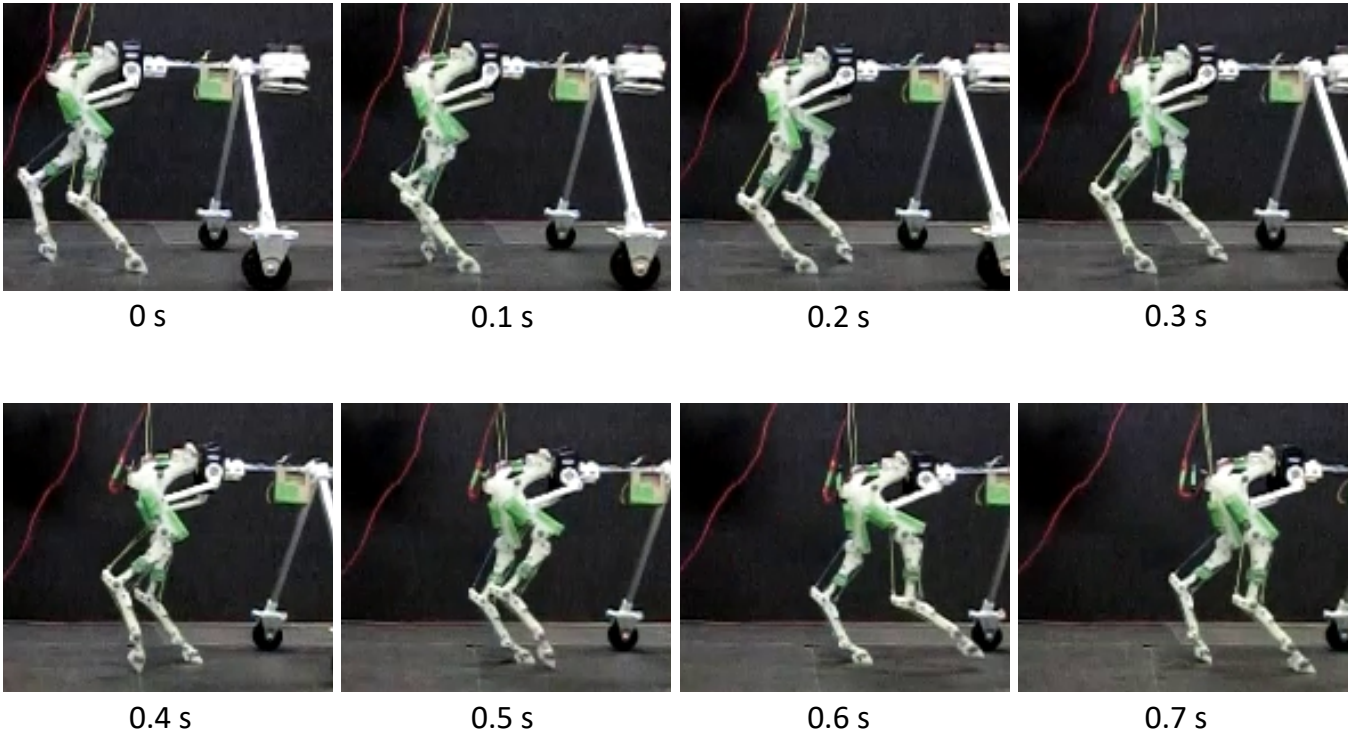|			
0 s	0.1 s	0.2 s	0.3 s
0.4 s	0.5 s	0.6 s	0.7 s

Fig. 8. Snapshots of the walking robot. The first 5 snapshots depict the stance phase of the right hindlimb. The following 3 snapshots depict the swing phase of the right hindlimb.

TABLE I

LENGTH OF BONES OF HORSE AND ROBOT

	Horse [mm]	Robot [mm]	Ratio
Tibia	383.5	97.2	3.96
Metatarsus	367.5	93.6	3.93
Mean	-	-	3.94

TABLE II

WEIGHT AND PERCENTAGE OF HINDLIMB SEGMENT

	Horse		Robot	
	[kg]	[%]	Target weight [g]	Measured weight [g]
Hindlimb	42.8	8.43	703	464
Femur	34.7	6.82	569	325
Tibia	4.8	0.95	79	78
Metatarsus	2.0	0.40	33	34
Pastern	1.3	0.26	22	13
Hoof				14
Head & Neck	57.7	11.4	950	820
Body weight	508.3	-	8337	2896

D. Weight ratio of each body parts

In order to reproduce the dynamics of the horse hindlimb, the weight ratio of each part of the leg was adjusted to the real horse's weight ratio. Additionally, when only the hindlimbs get weights, the center of gravity of the entire robot is greatly shifted backward. Therefore, we also set the weight of the head to adjust the center of gravity. In this study, we estimated the target weight of the robot using the geometric similarity, and based on that, designed the weight of each part of the hindlimb so that the weight ratio of each part would be equivalent to the real horses. The real size and weight of each part of the horse were taken from the literature [15]. We used the mean ratio between the lengths of the tibia and metatarsus to estimate the dimension ratio between the horse and the robot. Table I shows the dimensions and ratios of the horse, robot tibia, and metatarsus.

We estimated the target weight of each part of the robot by applying the geometric similarity to the obtained dimension ratio. Table II shows the weight and ratio of each part of the horse to the total weight, together with the target and measured values of the robot weight. Below the tibia, the measured weights of the robot and the target weights are similar. Although there is a difference between the target weight and the measured weight of the femur, the influence is considered to be small because the femur is driven by the servo motor directly. We set the weight of the head lighter than the target weight according to the weight of the hindlimb. Although there is a large difference between the weight of the entire robot and the target weight, as described above, the main purpose of setting the weight is to reproduce the dynamics of hindlimb and adjust the center of gravity of the entire robot. Thus, the total weight of the robot is not adjusted significantly. We will investigate the effect of the weight of the whole robot in detail in subsequent studies.

IV. EXPERIMENTS AND RESULTS

In this section, we present the walking experiments using the developed robot shown in section III. We verified that the walking motion of the robot can be simply generated by
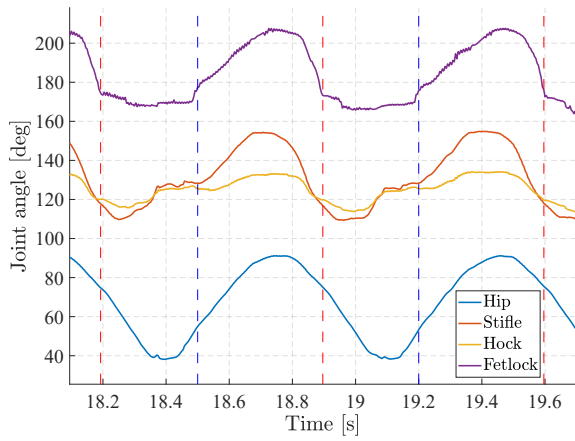
Fig. 9. The joint angles of the right hindlimb during walking. The blue break lines indicate touchdown timing. The red break lines indicate liftoff timing.

(a) Hip joint   (b) Stifle joint

(c) Hock joint   (d) Fetlock joint

Fig. 10. The joint angles of the right hindlimb during one stride. 0 s mean liftoff times. The blue lines indicate regular pattern (n = 13) . The red lines indicate failure pattern (n = 5) .

swinging the femur. Thereafter, we validated the contribution of the joint interlocking mechanisms to the emergence of the limb trajectory by comparing the joint angles between successful and failed walking.

A. Experimental setup

We measured the joint angles with a motion capture system. Seven markers for motion capture were attached to the center of rotation of each joint together with the tip of the hoof of the right hindlimb, and the waist. The touchdown and liftoff timing were judged by the marker attached to the tip of the hoof. The success of walking and the failure time were judged from the height of the marker attached to the waist. The experiments were conducted on a non-slip lane in order to prevent the robot hoof from slipping.

B. Movement of walking robot

Fig. 8 shows snapshots of the walking robot. The robot generated steady walking motion with a smooth transition between the swing and stance phases.

Fig. 9 shows the joint angles of the right hindlimb during walking. The robot generates completely different limb trajectories between the swing phase and the stance phase, such that all joints flex in the swing phase and extend in the stance phase. Furthermore, there are differences in the range of movement and the nature of interlocking even when compared to the movement by hand (Fig. 6) . In particular, the fetlock joint moves only 30 deg when moved by hand. In contrast, that joint moves more than 40 deg while walking. Moreover, the range of the movement of the fetlock joint extends to an angle that was not seen when the femur was moved by hand. This may be because it was extended by the ground reaction force applied to the hoof.

C. Comparison of regular pattern and failure pattern

Fig. 10 shows the joint angles of each joint during one stride when walking is successful and when walking has failed. When walking is successful, each joint of the limb
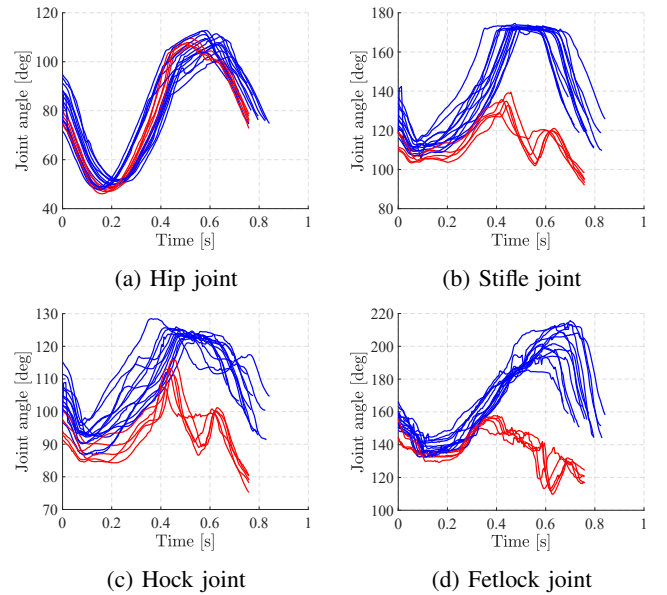
extends and the body is supported after the touchdown for about 0.2 seconds. Whereas, when walking has failed, the extension of the fetlock joint was for some reason inhibited around 0.4 seconds, and at the same time, the extension of other joints was also inhibited. As a result, the robot could not support its body weight. Thus, the robot fell over with sharp flexion of the stifle, hock, and fetlock joints. Possible causes of extension failure of the fetlock joint include, for example, the fact that the waist is too high and the hoof cannot contact the ground, or the angle of the fetlock joint at the time of touchdown is small and the hoof cannot properly receive the ground reaction force. This result shows that the function of the limb switches from swinging the entire limb to supporting the weight by receiving a ground reaction force.

V. CONCLUSIONS

This study focuses on the role of the interlocking mechanisms arising from the muscle-tendon structure of horses. We developed a robot with two hindlimbs, and as a result of walking experiment, the robot with the interlocking mechanism autonomously generated steady walking motion with a smooth transition between the swing and stance phases by simply swinging the hip joint with sinusoidal input. The comparison between successful and failed steps indicated that the function of the body support during stance phase was generated by the extension of the fetlock joint due to the interaction with the ground.

Future studies can improve the robot motion by adjusting the tendon lengths and body weights of horses. Furthermore, the movement of the robot can be evaluated by comparing it with the movement of a real horse. Moreover, we plan to develop a horse forelimb using the same procedure as we in the case of the hindlimb; we shall analyze the forelimb

movement and the movements when hindlimbs and forelimbs are combined.

REFERENCES

[1] L. Ren, M. Butler, C. Miller, H. Paxton, D. Schwerda, M. S. Fischer, and J. R. Hutchinson, "The movements of limb segments and joints during locomotion in african and asian elephants," *Journal of Experimental Biology*, vol. 211, no. 17, pp. 2735–2751, 2008.

[2] W. Back, H. C. Schamhardt, H. H. C. M. Savelberg, A. J. Van Den Bogert, G. Bruin, W. Hartman, and A. Barneveld, "How the horse moves: 1. significance of graphical representations of equine forelimb kinematics," *Equine Veterinary Journal*, vol. 27, no. 1, pp. 31–38, 1995.

[3] N. R. Deuel, "Coordination of equine forelimb motion during the gallop," *Equine Veterinary Journal*, vol. 26, no. S17, pp. 29–34, 1994.

[4] P. Carlson-Kuhta, T. V. Trank, and J. L. Smith, "Forms of forward quadrupedal locomotion. ii. a comparison of posture, hindlimb kinematics, and motor patterns for upslope and level walking," *Journal of Neurophysiology*, vol. 79, no. 4, pp. 1687–1701, 1998.

[5] J. L. Smith, P. Carlson-Kuhta, and T. V. Trank, "Forms of forward quadrupedal locomotion. iii. a comparison of posture, hindlimb kinematics, and motor patterns for downslope and level walking," *Journal of Neurophysiology*, vol. 79, no. 4, pp. 1702–1716, 1998.

[6] T. McGeer, "Passive dynamic walking," *The International Journal of Robotics Research*, vol. 9, no. 2, pp. 62–82, 1990.

[7] Y. Masuda and M. Ishikawa, "Autonomous intermuscular coordination and leg trajectory generation of physiology-based quasi-quadruped robot," in *IEEE/SICE International Symposium on System Integration (SII 2020)*, 2020, Accepted.

[8] W. Back, H. C. Schamhardt, H. H. C. M. Savelberg, A. J. Van Den Bogert, G. Bruin, W. Hartman, and A. Barneveld, "How the horse moves: 2. significance of graphical representations of equine hind limb kinematics," *Equine Veterinary Journal*, vol. 27, no. 1, pp. 39–45, 1995.

[9] K. M. Dyce, W. O. Sack, and C. J. G. Wensing, *Textbook of Veterinary Anatomy*, 3rd ed. Saunders, 6 2002. [Online]. Available: http://amazon.co.jp/o/ASIN/0721689663/

[10] P. R. Van Weeren, M. O. Jansen, A. J. Van den Bogert, and A. Barneveld, "A kinematic and strain gauge study of the reciprocal apparatus in the equine hind limb," *Journal of biomechanics*, vol. 25, no. 11, pp. 1291–1301, 1992.

[11] M. Hildebrand, "The mechanics of horse legs," *American Scientist*, vol. 75, no. 6, pp. 594–601, 1987.

[12] R. C. Payne, J. R. Hutchinson, J. J. Robilliard, N. C. Smith, and A. M. Wilson, "Functional specialisation of pelvic limb anatomy in horses (equus caballus)," *Journal of Anatomy*, vol. 206, no. 6, pp. 557–574, 2005.

[13] E. Goldfinger, *Animal Anatomy for Artists: The Elements of Form*. Oxford Univ Pr, 11 2004. [Online]. Available: http://amazon.co.jp/o/ASIN/0195142144/

[14] W. Back, H. C. Schamhardt, and A. Barneveld, "Are kinematics of the walk related to the locomotion of a warmblood horse at the trot?" *Veterinary Quarterly*, vol. 18, no. sup2, pp. 79–84, 1996.

[15] K. Kubo, T. Sakai, H. Sakuraoka, and K. Ishii, "Segmental body weight, volume and mass center in thoroughbred horses," *Japanese Journal of Equine Science*, vol. 3, no. 2, pp. 149–155, 1993.